doi: 10.1111/j.1365-3121.2009.00908.x

New thermochronometric constraints on the rapid Palaeogene exhumation of the Cordillera Darwin complex and related thrust sheets in the Fuegian Andes

David J. Gombosi,[1] David L. Barbeau Jr[1] and John I. Garver[2]

[1]*Tectonics & Sedimentation Laboratory, Department of Earth and Ocean Sciences, University of South Carolina, Columbia, SC 29208, USA;* [2]*Geology Department, Union College, Schenectady, NY 12308, USA*

ABSTRACT

Thermal modelling of new fission-track and (U–Th–Sm)/He data from the Fuegian Andes reveals rapid cooling (~12–48 °C Ma^{-1}) during the middle and late Eocene followed by slow cooling (~1.5 °C Ma^{-1}) to the Recent. We interpret the rapid cooling as a result of exhumation from contractional uplift within the crystalline interior of the orogen. This interpretation is consistent with independent evidence of Eocene shortening, flexural subsidence and provenance changes in the study area, and is approximately coeval with marine geochemical evidence of the onset of Drake Passage opening. In light of the Palaeogene history of Nazca-South American plate convergence and the differences in shortening magnitudes and exhumation histories between the Fuegian and Patagonian Andes, our data support Eocene development of the Patagonian orocline, which also provides a plausible explanation for early opening of Drake Passage.

Terra Nova, 21, 507–515, 2009

Introduction

The Fuegian Andes form a principal component of the Scotia Arc (Fig. 1), whose widely debated tectonic history has implications for several geological phenomena associated with opening of Drake Passage (Lawver and Gahagan, 2003; Eagles *et al*., 2005; Livermore *et al*., 2005, 2007), including ocean circulation and polar glaciation (Kennett, 1977; Barker and Thomas, 2004) and the interchange of fauna between Gondwanan continents (Regüero *et al*., 2002; Evans *et al*., 2008).

One remarkable aspect of the Fuegian Andes is their east–west orientation, which is in marked contrast to the north–south trend of the Patagonian Andes. Within the Fuegian Andes reside a suite of amphibolite and greenschist facies rocks known as the Cordillera Darwin complex (Fig. 1), which is in fault contact with lower-grade rocks along its margins (Klepeis, 1994a; Kohn *et al*., 1995). Because of its position near the change in orogenic strike of the Andes and its exceptionally high metamorphic grades, the Cordillera Darwin complex should provide unique insight into the tectonic history of the northern margin of the Scotia Arc.

Correspondence: David J. Gombosi, Department of Earth Sciences, Syracuse University, 204 Heroy Geology Lab, Syracuse, NY 13244, USA. Tel.: +1 781 789 9718; e-mail: djgombos@syr.edu

To constrain the low-temperature thermochronology of the Fuegian Andes, we report temperature–time (*T*–*t*) pathways constructed from new apatite and zircon fission-track and (U–Th–Sm)/He data from the Cordillera Darwin complex and adjacent rocks. Nelson (1982) determined fission-track ages from the Cordillera Darwin complex and rocks south of the Beagle Channel, which Kohn *et al*. (1995) integrated with $^{40}Ar/^{39}Ar$ ages to reveal two broad pulses of cooling from 90 to 70 Ma and from 60 to 40 Ma. Advances in low-temperature thermochronometry achieved since the previous studies (e.g. Fitzgerald *et al*., 1995; Gallagher *et al*., 1998; Farley, 2002; Ehlers *et al*., 2005; Ketcham, 2005) allow us to examine lower temperature processes, better constrain thermal pathways, incorporate kinetic parameters, and interpret multiple populations of cooling ages from individual samples. With this new perspective, we re-examine the exhumation history of the Fuegian Andes with an eye towards assessing the orogen's temporal and possibly kinematic relationship to the opening of the adjacent Drake Passage.

Geological background and setting

The leading (Pacific) margin of the southernmost Andes is composed of an Upper Jurassic–Neogene magmatic arc and accretionary prism (Hervé *et al*., 2007). North and east of the magmatic arc, amphibolite-grade metasedimentary strata of the Cordillera Darwin complex comprise the most elevated and deeply exhumed units of the Fuegian Andes (Nelson *et al*., 1980; Kohn *et al*., 1993; Cunningham, 1995). This Upper Paleozoic–Lower Mesozoic accretionary prism was amalgamated to the South American margin during the Gondwanide orogeny (Hervé *et al*., 2003, 2008), buried to 20-km depths following emplacement of the Jurassic Darwin intrusive suite and Tobífera Formation volcanic strata associated with the break-up of Gondwana (Mukasa and Dalziel, 1996; Pankhurst *et al*., 2000) and exhumed during the Cretaceous and Palaeogene (Nelson, 1982; Kohn *et al*., 1995).

In presumed thrust fault contact with the Cordillera Darwin complex are Jurassic and Lower Cretaceous ophiolitic, volcanic and associated sedimentary rocks that accumulated in the Rocas Verdes basin inboard of the coeval magmatic arc (Suárez and Pettigrew, 1976; Bruhn *et al*., 1978; Dalziel, 1981). Cretaceous–Palaeo-

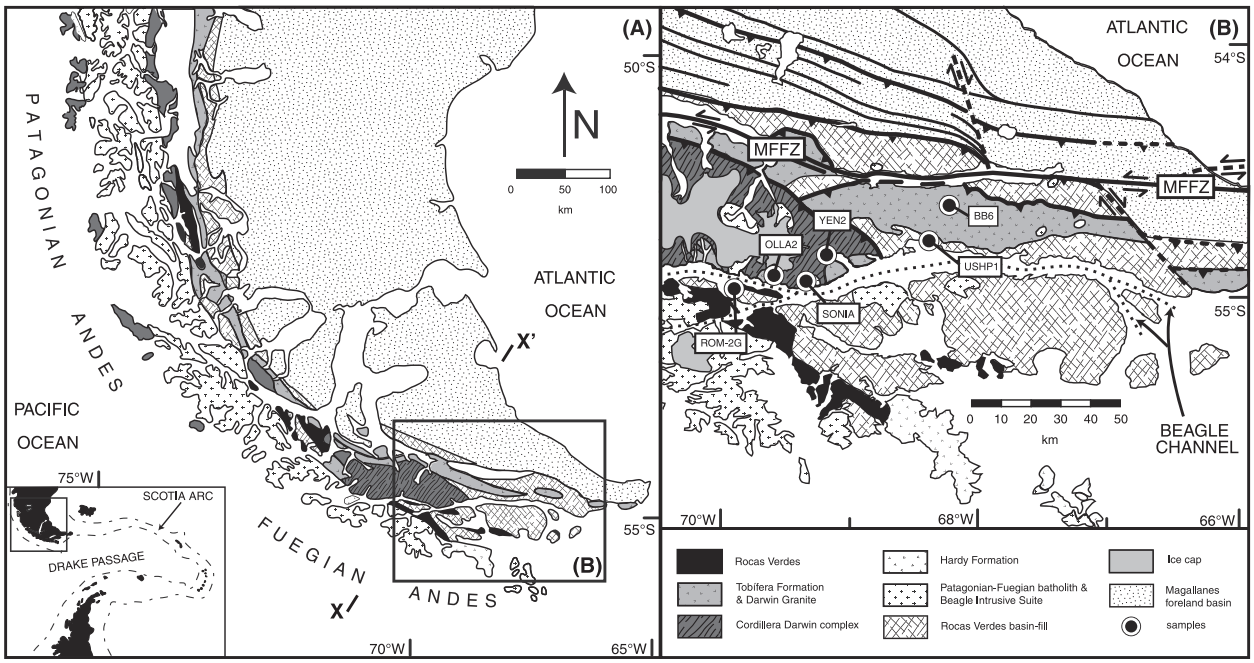

Fig. 1 Simplified geological maps of the southern Andes. (A) Patagonian and Fuegian Andes, modified from Wilson (1991) and Fildani and Hessler (2005). Schematic cross-section from X to X′ occurs in Fig. 4. (B) Eastern Fuegian Andes showing location of thermochronology samples. Geology compiled from Nelson *et al.* (1980), Wilson (1991), Kohn *et al.* (1993, 1995), Klepeis (1994a,b), Olivero and Malumián (2008) and fieldwork conducted by the first two authors. MFFZ, Magallanes–Fagnano fault zone.

gene inversion of this basin imbricated the Fuegian hinterland (Klepeis, 1994a; Kraemer, 2003; Menichetti *et al.*, 2008), loading the adjacent crust to form the Magallanes foreland basin (Biddle *et al.*, 1986; Olivero and Malumián, 2008), which was progressively incorporated into the orogen through Palaeogene shortening (Klepeis, 1994a; Ghiglione and Ramos, 2005; Olivero and Malumián, 2008).

Structural relationships along the northern margin of Cordillera Darwin complex indicate that the complex experienced north-vergent thick-skinned thrusting over a footwall composed of Jurassic Tobífera Formation and Lower Cretaceous strata of the Rocas Verdes basin (Klepeis, 1994a). The nature of the southern contact between the Cordillera Darwin complex and lower-grade rocks south of the Beagle Channel is debated (Dalziel and Brown, 1989; Klepeis, 1994a), but recent research favours south-vergent thrusting (Klepeis *et al.*, 2008).

In the early Neogene, convergence and shortening decreased coincidently with the development of the sinistral Magallanes–Fagnano fault system (Klepeis, 1994b).

Methods

In this study, we analysed zircon and apatite through fission-track and (U–Th–Sm)/He thermochronology from crystalline rock of the Cordillera Darwin complex and adjacent units (Fig. 1, Appendix S1). Upon crystallization of zircon and apatite, spontaneous fission of ^{238}U causes recoil damage to the crystal lattice producing fission tracks, while alpha decay of ^{238}U, ^{235}U, ^{232}Th and ^{147}Sm produces ^{4}He. Fission tracks anneal above mineral-specific closure temperatures of ~225–250 °C for zircon (Brandon *et al.*, 1998) and ~110–125 °C for apatite (Ketcham *et al.*, 1999) in rapidly cooled minerals. Similarly, ^{4}He diffuses out of the studied crystals above ~170–190 °C for zircon (Reiners *et al.*, 2004) and ~55–80 °C for apatite (Farley, 2000). Below these temperatures, daughter products are retained, thereby recording the time elapsed since system closure.

We constrained the cooling ages of our collected samples using standard sample preparation and analytical routines (Appendix S2). A chi-squared test was performed on all zircon fission-track (ZFT) and apatite fission-track (AFT) data. If a population revealed over-dispersion indicated by a chi-squared value of $< 5\%$ (Galbraith, 1981) we performed a binomial peak fitting routine on the data (*Binomfit*: Brandon, 1992, 1996) to constrain the multiple populations. Often, this over-dispersion is a result from long residence times within or near the partial annealing zone (Fitzgerald *et al.*, 1995), which forces grains with slightly different annealing kinetics to distinguish themselves in different groups.

Results

Fission-track results are presented in Table 1 and Appendices S3–S6; (U–Th–Sm)/He results are presented in Table 2 and Appendices S7–S8. Figure 2 depicts modelling of multimodal cooling-age populations acquired from ZFT data from two samples. All reported errors in the main text are at the 1σ level, except for multi-component modelling efforts

Table 1 Zircon and apatite fission-track results.

Sample	N_s	ρ_s (10^6 t cm^{-2})	N_i	ρ_i (10^6 t cm^{-2})	N_d	ρ_d (10^5 t cm^{-2})	n	χ^2 (%)	Age (Ma, 1σ)	Mean length and Dpar (μm, 1σ)	Mean *U* (p.p.m., 2σ)
Cordillera Darwin complex											
SONIA1 (ZFT)	538	5.88	484	5.32	1970	2.416	13	21	46.1−3.1/+3.4	N/A	270.4 ± 26.9
YEN2 (ZFT)	780	6.96	807	7.20	1959	2.403	15	29.4	41.1−2.4/+2.6	N/A	368.7 ± 30.2
OLLA2 (ZFT)	587	13.9	546	12.9	1968	2.435	11	30.5	46.2−3.0/+3.2	N/A	655.6 ± 61.9
Felsic pluton from Isla Gordon											
ROM-2G (ZFT)	2668	5.47	1637	33.6	1970	2.442	30	1.2	70.3−3.1/+3.2	N/A	169.1 ± 10.6
ROM-2G (AFT)	270	0.29	N/A	N/A	N/A	N/A	25	27.8	44.8 ± 3.1	1.72 ± 0.17, 13.52 ± 1.69	19.54 ± 18.8
Volcanic strata from footwall of Cordillera Darwin basement thrust											
BB6 (ZFT)	2586	9.26	2059	7.33	1972	2.449	33	0.5	54.4−2.3/+2.4	N/A	368.4 ± 21.4

N_s, N_i, N_d, and ρ_s, ρ_i, ρ_d are the number and density of spontaneous, induced and dosimeter tracks respectively. n is the number of grains counted; χ^2 is the chi-squared probability. Fission-track ages were determined using the zeta method (Hurford and Green, 1983) and ages were calculated using computational protocols from Brandon (1992). A zeta factor of 355.1 ± 9.4 (1σ) for DJG was based on standard calibrations of the Fish Canyon Tuff, Buluk Tuff, and Peach Springs Tuff (Appendix S3) using the external detector method and CN5 as the dosimeter glass. All reported ages are pooled ages when $\chi^2 \geq 5\%$; otherwise chi-squared ages are reported. Fission-track analysis on apatite resulted in a zeta factor of 13.475 ± 0.341 (1σ), for P. O'Sullivan was based on standard calibrations of the Durango Apatite, Tioga standard, Fish Canyon Tuff, and Mount Dromedary Apatite. This zeta factor for P. O'Sullivan was significantly different from DJG, due to the fact an LA-ICP-MS was used to directly measure [U]. All ages are listed as pooled ages. Etched pit parameters of Dpar (Donelick, 1993) were measured to constrain annealing kinetics. See Appendices S4–S5 for individual [U] and track counts and Appendix S6 for track length data.

Table 2 Zircon and apatite (U–Th–Sm)/He results.

Sample	Mwar (μm)	Mass (μg)	U (p.p.m.)	Th (p.p.m.)	Sm (p.p.m.)	Th/U	^{4}He (nmol g^{-1})	F_T	Corrected age (Ma)	Mean age (Ma)	Total error (Ma, 1σ)
Cordillera Darwin complex											
SONIA5g-A1	45.25	2.61	7.73	5.87	80.65	0.76	0.51	0.69	14.78	15.34	2.10
SONIA5g-A2	48.50	3.63	8.39	7.12	79.72	0.85	0.69	0.72	17.64		
SONIA5g-A3	41.75	1.92	17.97	37.68	49.99	2.10	1.30	0.66	13.59		
SONIA1-Z1	43.25	4.17	392.17	275.01	–	0.70	68.53	0.76	36.65	37.95	2.33
SONIA1-Z3	42.25	3.32	530.88	437.83	–	0.82	100.05	0.74	39.25		
YEN2-Z1	58.00	12.98	287.97	95.820	–	0.33	53.31	0.83	38.46	39.44	2.91
YEN2-Z2	55.75	8.24	288.23	101.53	–	0.35	53.46	0.81	39.25		
YEN2-Z3	61.50	10.90	276.94	94.980	–	0.34	54.10	0.82	40.60		
OLLA2-Z1	31.75	1.67	1621.9	897.13	–	0.55	264.84	0.68	39.25	42.41	6.28
OLLA2-Z2	22.50	0.58	1556.2	916.28	–	0.59	210.76	0.57	38.83		
OLLA2-Z3	29.50	0.99	1987.8	1088.0	–	0.55	375.86	0.63	49.15		
Felsic pluton from Isla Gordon											
ROM-2G-A1	68.25	5.38	12.35	36.34	39.12	2.94	1.09	0.78	12.36	20.05	11.70
ROM-2G-A2	54.25	4.66	11.21	23.91	27.65	2.13	1.08	0.75	15.74		
ROM-2G-A3	41.75	2.05	9.85	4.09	80.53	0.42	1.27	0.67	32.05		
ROM-2G-Z1	77.65	–	–	–	–	0.62	–	–	44.20	46.25	3.36
ROM-2G-Z2	56.34	–	–	–	–	0.67	–	–	48.30		
Footwall to Cordillera Darwin basement thrust											
BB6-Z1	38.00	2.92	575.45	334.80	–	0.58	120.38	0.73	46.63	43.80	3.50
BB6-Z2	28.00	1.34	280.85	176.78	–	0.63	48.13	0.65	42.36		
BB6-Z3	38.50	5.16	347.48	169.54	–	0.49	66.97	0.75	42.41		
USHP1-A1	37.50	1.55	11.45	46.94	106.76	4.10	1.22	0.66	15.14	14.56	0.77
USHP1-A2	32.25	1.20	14.60	66.84	146.22	4.58	1.42	0.58	14.77		
USHP1-A3	39.50	1.84	15.47	65.38	175.29	4.23	1.56	0.67	13.79		
USHP1-Z1	44.75	4.92	903.53	517.92	–	0.57	209.74	0.77	49.16	46.38	4.21
USHP1-Z2	43.75	3.98	1039.9	695.72	–	0.67	231.36	0.76	47.01		
USHP1-Z3	39.75	2.47	1590.3	674.97	–	0.42	293.44	0.72	42.96		

Samples with a '-Z#' suffix are zircon; samples with a '-A#' suffix are apatite. Analysis follows the method of Reiners and Nicolescu (2006). Alpha-ejection corrections for all samples with the exception of ROM-2G followed Farley (2002), House *et al.* (2000) and Reiners and Nicolescu (2006). Alpha-ejection corrections for ROM-2G zircons followed Gombosi *et al.* (2008): each grain was polished, converted to a spherical equivalent geometry, and then corrected using the method of Hourigan *et al.* (2005). 'Mwar' is the mean weighted average radius, the geometrical equivalent of a sphere with the equivalent surface area to volume ratio; F_T is the alpha-ejection correction coefficient. Each individual sample constitutes a single-grain aliquot.

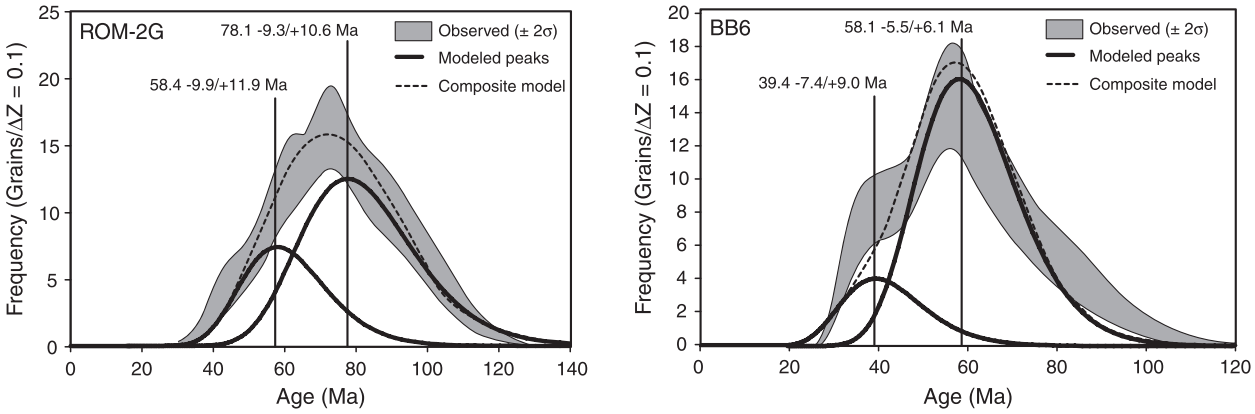

Fig. 2 Results of modelling of over-dispersed zircon fission-track ages from samples BB6 and ROM-2G into multiple component distributions via binomial peak fitting (Galbraith and Green, 1990; Brandon, 1992, 1996). Vertical lines indicate approximate positions of peaks of best-fit age distributions. The ages and 2σ errors of best-fit age peaks are labelled.

in which case errors are reported at the 2σ level.

Cordillera Darwin complex

The low-temperature history of analysed Cordillera Darwin complex samples SONIA, YEN2 and OLLA2 is recorded by ZFT ages spanning ca. 49–38 Ma and zircon (U–Th–Sm)/He (ZHe) ages of *c*. 49–36 Ma. A single apatite (U–Th–Sm)/He (AHe) age of 15.3 ± 2.1 Ma was obtained from SONIA.

Felsic pluton from Isla Gordon

Zircon fission-track and ZHe data from sample ROM-2G yielded cooling ages of 70.3−3.1/+3.2 and 46.3 ± 3.4 Ma respectively. AFT data yielded a 44.8 ± 3.1 Ma cooling age with a mean track length of 13.52 ± 1.69 μm; AHe data yielded ages spanning 30–10 Ma. The large age range for the AHe ages is associated with a single grain with a 10–20 Ma disparity from other ages in the sample. Elimination of this grain from analysis yields significantly improved precision with a 77% reduction in scatter, although all ages were included in our *T–t* modelling (Fig. 3).

Analysis of ZFT data indicates that the plutonic sample ROM-2G fails the chi-squared test, which we tentatively attribute to variable radiation damage (Garver *et al.*, 2005) on account of a weak inverse correlation between [U] and ZFT age (Appendix S4). It is possible that this over-dispersion was amplified because of prolonged residence of the sample in the zircon partial annealing zone, which would give zircons with slightly different annealing kinetics sufficient time to deviate into two different populations.

When modelled as a multi-component system, the ROM-2G age data (Fig. 2) reveal two populations of 58.4−9.9/+11.9 Ma and 78.1−9.3/+10.6 Ma; we interpret the younger population as the most recent significant period of cooling.

Cordillera Darwin basement-thrust footwall

Zircon fission-track analysis of metavolcaniclastic sample BB6 from the Cordillera Darwin basement-thrust footwall (*sensu* Klepeis, 1994a) fails the chi-squared test, which we interpret to have similar root causes as in ROM-2G (Appendix S4). Modelling revealed two populations: one with a ZFT age of 39.4−7.4/+9.0 Ma, interpreted as the cooling age, with a subsidiary population at 58.1−5.5/+6.1 Ma (Fig. 2). ZHe data from samples USHP1 and BB6 yielded cooling ages of 46.4 ± 4.2 and 43.8 ± 3.5 Ma, respectively, whereas AHe data from USHP1 yielded a cooling age of 14.6 ± 0.8 Ma.

Thermal modelling

By recording the timing of passage of an individual sample through different isotherms, the multiple-thermochronometer approach constrains average cooling rates between closure temperatures, which can identify periods of rapid cooling caused by exhumation and rock-uplift (Nelson, 1982; Reiners *et al.*, 2000). With a presumed or measured relationship between depth and temperature in the crust, the resulting *T–t* pathways can be used to estimate average exhumation rates. In Fig. 3, we present the results of HeFTy Monte Carlo simulations (Ketcham, 2005) of our cooling ages and related kinetic data that depict plausible *T–t* pathways for each sample. Figure 4 summarizes our interpretations of the modelling results. Details of the modelling parameters and the parameters for calculating closure temperatures are included in Appendix S2.

Discussion

1 Modelling of our new thermochronometry data from the Fuegian Andes hinterland reveals rapid cooling (averaging ~12–48 °C Ma^{-1}) during the middle and late Eocene, followed by slow cooling of ~1.5 °C Ma^{-1} to the Recent (Fig. 3). Samples OLLA2 and ROM-2G indicate an onset of rapid cooling at *c*. 48 Ma, which is consistent with pathways from samples SONIA, YEN2 and BB6 that record rapid exhumation beginning no later than 45 Ma. Modelled *T–t* pathways suggest a cessation of this rapid cooling by *c*. 34 Ma. These results indicate a more rapid-cooling history than recognized by previous efforts (Nelson, 1982;

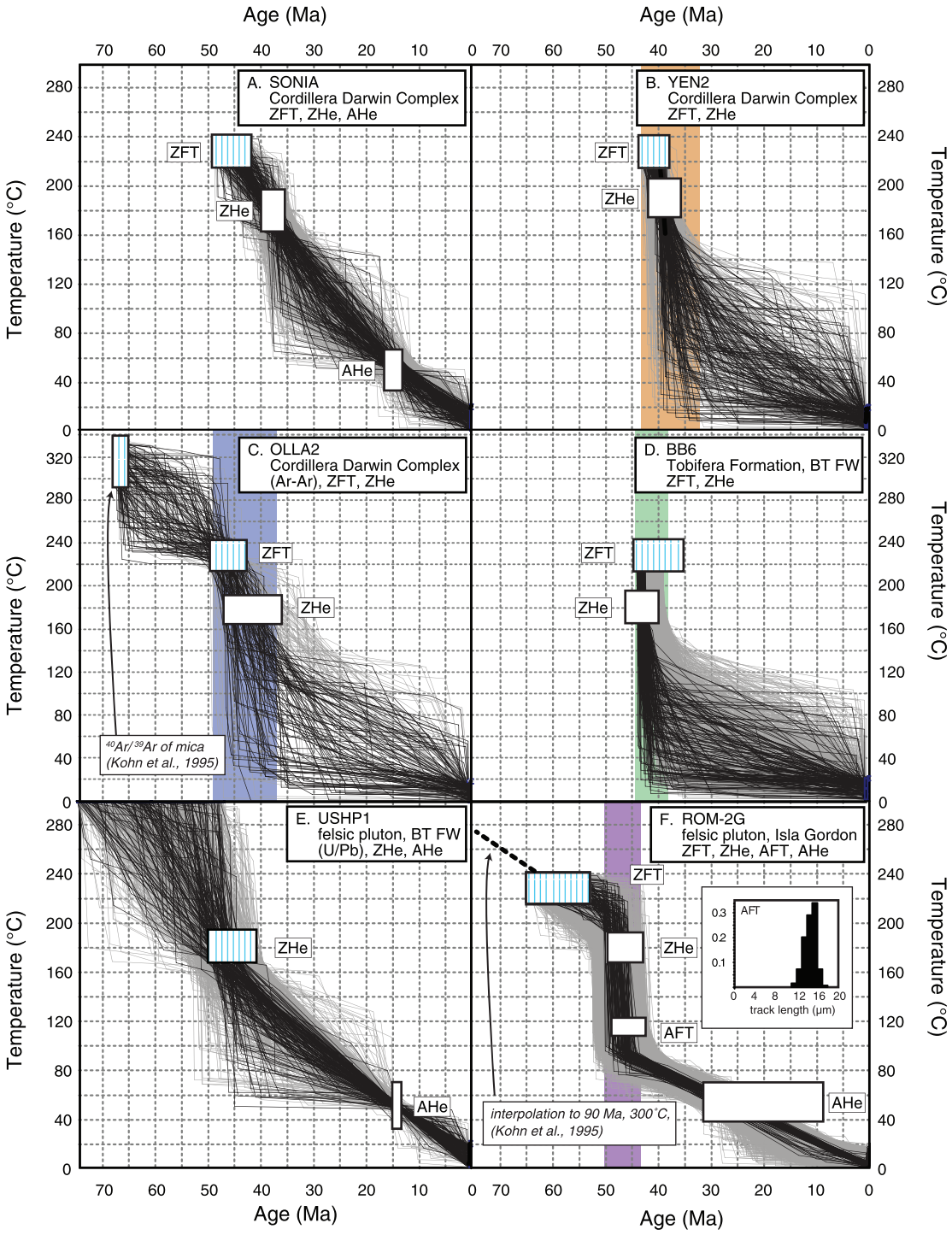

Fig. 3 Inverse models of *T*–*t* pathways for samples collected from the Fuegian Andes. White boxes with vertical blue dashed lines represent a priori constraints from ZFT or $^{40}Ar/^{39}Ar$ data which the *T*–*t* paths were forced through. The white boxes represent approximate locations of other thermochronometers for which individual closure temperatures were calculated during each model iteration. Black lines reveal model pathways with goodness-of-fit (GOF: Ehlers *et al.*, 2005) >0.5, while those in grey have GOF of <0.5 but >0.05. Coloured boxes bracket periods of maximum exhumation rates determined by eye from each model. All errors in the inverse model are at the 1σ level.

Kohn *et al.*, 1995) and more tightly bracket the onset and cessation of rapid Palaeogene cooling (Fig. 4).

2 Assuming geothermal gradients of 25–50 °C km^{-1}, the rapid-cooling periods represented by our data yield averaged exhumation rates of ~0.5–1.1 mm yr^{-1} that were sustained for >5 Ma (Figs 3 and 4),

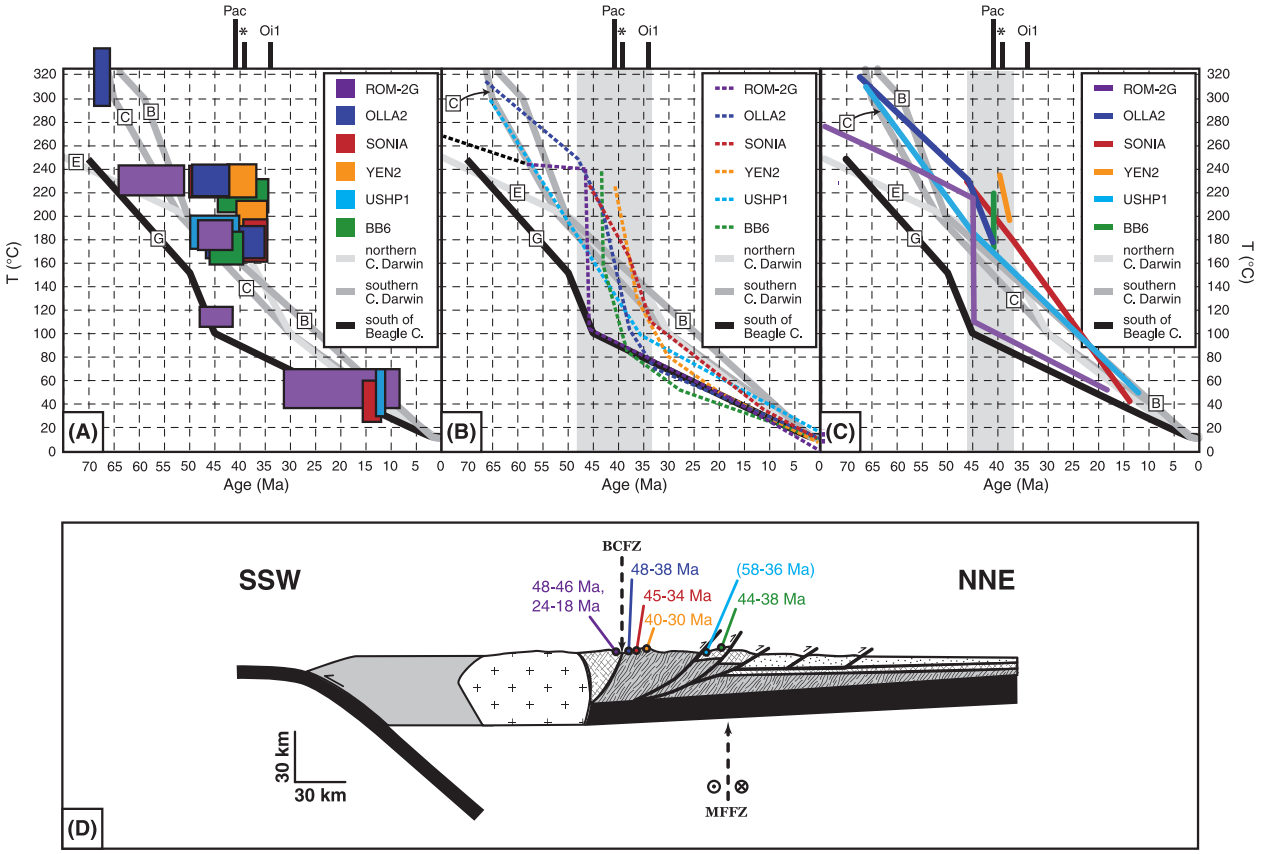

Fig. 4 Summary of thermochronological results from Fuegian Andes. (A) New thermochronometric data and errors presented herein are indicated by coloured polygons. Labelled black and grey pathways correspond to *T*–*t* pathways for separate areas of the Cordillera Darwin region reported in Kohn *et al.* (1995), which incorporate fission-track data from Nelson (1982). Pac: arrival of water-mass with juvenile Nd-isotope signature in the Atlantic sector of the Southern Ocean signifying opening of Drake Passage to marine throughflow (Scher and Martin, 2006), Oi1: earliest Oligocene glaciation of Antarctica, *dramatic sediment provenance shift in the eastern Magallanes foreland basin (Barbeau *et al.*, 2009). (B) Best-fit *T*–*t* pathways constructed from the graphical middle of HeFTy Monte Carlo simulation envelopes with GOF > 0.5. These lines are meant to be suggestive of one of possibly many 'good' paths. Grey polygons depict periods of rapid exhumation of the study area. (C) *T*–*t* pathways constructed from interpolation of data in (A). Grey polygons depict periods of rapid exhumation of the study area. (D) Simplified cross-section through the Fuegian Andes annotated with periods of rapid exhumation indicated by modelling of individual samples' temperature-time pathways. Jurassic volcanic strata and those associated with the Rocas Verdes ophiolites and basin-fill are combined into a single tectonostratigraphic unit indicated by cross-hatched pattern. MFFZ, Magallanes–Fagnano fault zone; BCFZ, Beagle Channel fault zone.

on par with values recognized in other active modern and ancient orogens that expose upper and middle crustal rocks (Burbank, 2002). In contrast, the post-Eocene slow cooling recorded in our samples is equivalent to exhumation of ~0.02–0.05 mm yr^{-1}, similar to rates in quiescent (post-tectonic) orogens (Spotila, 2005). Although the faster cooling episodes recorded in our samples occurred at rates that are consistent with estimates for landslide, glacial, and fluvial erosion rates over timescales of 10^2–10^5 years (Burbank, 2002), isostatic and crustal thickness considerations argue against sustained exhumation (≥10^6 years) at these rates unless aided by contemporaneous rock-uplift. Thus, in light of the prolonged and high rates of erosion required by our data, we interpret our results to signify rapid Palaeogene exhumation caused by shortening and rock-uplift of the Fuegian Andes' hinterland.

3 The overlap of representative rapid-cooling segments demonstrated in Monte Carlo simulations (Figs 3 and 4B) and simple interpolations of cooling constraints (Fig. 4C) from our data suggests generally contemporaneous exhumation across the Fuegian Andes crystalline hinterland, including the Cordillera Darwin complex and lower-grade rocks in fault contact immediately to the north and south (Fig. 4D). Whereas further thermochronometric and structural analysis may allow the discrimination of the kinematics of individual thrust sheets, the significant overlap between Monte Carlo models for different samples currently precludes confident application of the

different cooling histories to a more detailed kinematic history of the orogenic wedge.

4 Our data contribute to mounting evidence for an apex of tectonic activity in the Scotia Arc during the middle and late Eocene. A pronounced water-mass provenance change recorded by the Nd-isotope composition of fossil fish teeth in the Atlantic sector of the Southern Ocean at *c*. 41 Ma marks the first significant opening of the Drake Passage marine gateway between South America and the Antarctic Peninsula (Scher and Martin, 2006), coincident with models for the development of the Dove and Protector basins (Eagles *et al*., 2006). The timing of this isotope shift and basin formation is approximately coincident with rapid exhumation in the Fuegian Andes indicated by the data presented herein, as well as by the dramatic sediment provenance shift at *c*. 39 Ma in the Magallanes foreland basin that Barbeau *et al*. (2009) interpreted as evidence of rock- and surface-uplift of the Cordillera Darwin complex and adjacent hinterland thrust sheets. Our new thermochronometry data corroborate the interpretation of Barbeau *et al*. (2009) and further support synchrony between the tectonics of the Fuegian Andes and opening of Drake Passage.

5 Although contemporaneous early opening of Drake Passage and rapid exhumation in the Fuegian Andes infers a possible genetic relationship between the regional tectonics of southernmost South America and one of the most significant Cenozoic reconfigurations of global ocean circulation (Barker, 2001; Lawver and Gahagan, 2003; Lagabrielle *et al*., 2009), the mechanics required for these coeval phenomena present a challenge. Whereas an extensional mechanism for middle to late Eocene uplift and exhumation of the Darwin Complex (e.g. Dalziel and Brown, 1989) is consistent with recent interpretation of Eocene extension to the east (Ghiglione *et al*., 2008) and subsequent seafloor spreading in the Scotia Sea (Barker, 2001), kinematic analysis of Cordillera Darwin and adjacent regions indicate a dominantly contractional Palaeogene history (e.g. Nelson, 1982; Wilson, 1991; Alvarez-Marrón *et al*., 1993; Klepeis, 1994a,b; Klepeis and Austin, 1997; Kraemer, 2003; Ghiglione and Ramos, 2005; Klepeis *et al*., 2008; Torres Carbonell *et al*., 2008). These structural interpretations are consistent with coeval flexural subsidence recorded in the Magallanes foreland basin (Biddle *et al*., 1986; Ghiglione and Ramos, 2005; Torres Carbonell *et al*., 2008), thus the rapid cooling recorded in our samples most likely occurred because of rock-uplift and exhumation caused by crustal shortening. If correct, the above interpretations of southern Andean tectonics and Drake Passage opening requires the seemingly incongruous scenario of convergence within the East–West oriented Fuegian Andes contemporaneous with divergence between the respective termini of southern South America and the Antarctic Peninsula.

We suggest that Eocene development of the Patagonian orocline by anticlockwise rotation of the Fuegian Andes relative to the Patagonian Andes could account for these phenomena. Structural reconstructions indicate 300–600 km of post-Jurassic shortening within the Fuegian segment of the orogenic belt in comparison with significantly less shortening in the Patagonian Andes (Kraemer, 2003; Giacosa and Heredia, 2004; Ghiglione and Ramos, 2005). In light of the later (Oligocene) onset of rapid exhumation in the Patagonian Andes (Thomson *et al*., 2001) and low pre-Oligocene convergence rates between the Nazca and South American plates at the latitudes of the Patagonian Andes (Somoza, 1998; Somoza and Ghidella, 2005), our new data combine with complementary evidence of middle to late Eocene peak shortening in the Fuegian Andes (Biddle *et al*., 1986; Ghiglione and Ramos, 2005; Torres Carbonell *et al*., 2008; Barbeau *et al*., 2009) to infer an Eocene development of the Patagonian orocline. Although vertical-axis rotation studies of this hypothesized orocline are currently equivocal (Rapalini, 2007) and analogue sandbox models have been used to suggest that the southern Andes may have been bent since the Cretaceous (Ghiglione and Cristallini, 2007), the co-occurrence of dramatic changes in shortening and orogenic strike between the Patagonian and Fuegian Andes at the approximate location of the most deeply exhumed rocks in the southern Andes is consistent with oroclinal bending (Marshak, 1988; Kraemer, 2003). If correct, such a model provides one explanation for simultaneous Eocene penetration of Pacific seawater through Drake Passage (Scher and Martin, 2006; Livermore *et al*., 2007) while causing the rapid exhumation in the Fuegian Andes recorded by our thermochronology data.

Acknowledgements

This research was supported by NSF grant ANT-0732995 and a USC Research & Productive Scholarship grant to DLB. K. Klepeis, M. Kohn, P. Reiners and N. Swanson-Hysell provided guidance in the interpretation of our data. N. Swanson-Hysell, K. Murray, K. Zahid, A. Moragues and P. Torres Carbonell assisted with sample collection. P. O'Sullivan conducted AFT analyses. S. Nicolescu and P. Reiners assisted with (U–Th–Sm)/He analyses. M. Montario and E. Enkelmann assisted with ZFT analyses. E. and M. Olivero provided logistic assistance and housing at the Centro Austral de Investigaciones Científicas (CADIC-CONICET), Argentina. M. D. and J. Darton provided invaluable guidance to DLB. Constructive reviews by S. Thomson, B. Heberer, Y. Lagabrielle and Associate Editor M. Rahn greatly improved the paper.

References

Alvarez-Marrón, J., McClay, K.R., Harambour, L.R. and Skarmeta, J., 1993. Geometry and evolution of the frontal part of the Magallanes foreland fold and thrust belt (Vicuña Area), Tierra del Fuego, Southern Chile. *AAPG Bull*., **77**, 1904–1921.

Barbeau, D.L., Olivero, E.B., Swanson-Hysell, N., Zahid, K.M., Murray, K.E. and Gehrels, G., 2009. Detrital-zircon geochronology of the eastern Magallanes foreland basin: Implications for late Eocene kinematics of the northern Scotia Arc and Drake Passage. *Earth and Planetary Science Letters*, **284**, 489–503.

Barker, P.F., 2001. Scotia Sea regional tectonic evolution: implications for mantle flow and paleocirculation. *Earth-Sci. Rev*., **55**, 1–39.

Barker, P.F. and Thomas, E., 2004. Origin, signature and paleoclimate influence of the Antarctic Circumpolar Current. *Earth-Sci. Rev.*, **66**, 143–162.

Biddle, K.T., Uliana, M.A., Mitchum, R.M., Jr, Fitzgerald, M.G. and Wright, R.C., 1986. The stratigraphic and structural evolution of the central and eastern Magallanes Basin, southern South America. In: *Foreland Basins* (P.A. Allen and P. Homewood, eds), *Int. Assoc. Sedimentol. Spec. Publ.*, **8**, 41–61.

Brandon, M.T., 1992. Decomposition of fission-trackgrain-age distributions. *Am. J. Sci.*, **292**, 535–564.

Brandon, M.T., 1996. Probability density plot for fission-track grain-age samples. *Radiat. Meas.*, **26**, 663–676.

Brandon, M.T., Roden-Tice, M.K. and Garver, J.I., 1998. Late Cenozoic exhumation of the Cascadia accretionary wedge in the Olympic Mountains, northwest Washington State. *Geol. Soc. Am. Bull.*, **110**, 985–1009.

Bruhn, R.L., Stern, C.R. and De Wit, M.J., 1978. Field and geochemical data bearing on the development of a Mesozoic volcano-tectonic rift zone and back-arc basin in southernmost South America. *Earth Planet. Sci. Lett.*, **41**, 32–46.

Burbank, D.W., 2002. Rates of erosion and their implications for exhumation. *Mineral. Mag.*, **66**, 25–52.

Cunningham, W.D., 1995. Orogenesis at the southern tip of the Americas: the structural evolution of the Cordillera Darwin metamorphic complex, southernmost Chile. *Tectonophysics*, **244**, 197–229.

Dalziel, I.W.D., 1981. Back-Arc extension in the southern Andes: a review and critical reappraisal. *Philos. Trans. R. Soc. Lond. A*, **300**, 1454, 319–335.

Dalziel, I.W.D. and Brown, R.L., 1989. Tectonic denudation of the Darwin metamorphic core complex in the Andes of Tierra del Fuego, southernmost Chile: implications for Cordilleran orogenesis. *Geology*, **17**, 699–703.

Donelick, R.A., 1993. *Method of Fission-Track Analysis Utilizing Bulk Chemical Etching of Apatite*. United States Patent No. 5,267,274.

Eagles, G., Livermore, R.A., Fairhead, J.D. and Brown, P., 2005. Tectonic evolution of the west Scotia Sea. *J. Geophys. Res.*, **110**, B02401–B02420.

Eagles, G., Livermore, R.A. and Morris, P., 2006. Small basins in the Scotia Sea: the Eocene Drake Passage gateway. *Earth Planet. Sci. Lett.*, **242**, 343–353.

Ehlers, T.A., Chaudhri, T., Kumar, S., Fuller, C.W., Willett, S.D., Ketcham, R.A., Brandon, M.T., Belton, D.X., Kohn, B.P., Gleadow, A.J.W., Dunai, T.J. and Fu, F.Q., 2005. Computational tools for low-temperature thermochronometer interpretation. In: *Low-Temperature Thermochronology: Techniques, Interpretations, and Applications* (P.W. Reiners and T.A. Ehlers, eds), *Rev. Mineral. Geochem.*, **58**, 49–94.

Evans, S.E., Jones, M.E. and Krause, D.E., 2008. A giant frog with the South American affinities from the Late Cretaceous of Madagascar. *Proc. Natl Acad. Sci. U.S.A.*, **105**, 2951–2956.

Farley, K.A., 2000. Helium diffusion from apatite: general behaviors as illustrated by the Durango fluorapatite. *J. Geophys. Res.*, **105**, 2903–2914.

Farley, K.A., 2002. (U-Th)/He dating: techniques, calibrations, and applications. In: *Noble Gases* (D.P. Porcelli, C.J. Ballentine and R. Wieler, eds). *Rev. Mineral. Geochem.*, **47**, 819–844.

Fildani, A. and Hessler, A.M., 2005. Stratigraphic record across a retroarc basin inversion: Rocas Verdes-Magallanes Basin, Patagonian Andes, Chile. *Geol. Soc. Am. Bull.*, **117**, 1596–1614.

Fitzgerald, P.G., Sorkhabi, R.B. and Redfield, T.F., 1995. Uplift and denudation of the central Alaska range: a case study in the use of apatite fission track thermochronology to determine absolute uplift parameters. *J. Geophys. Res.*, **100**, 20175–20191.

Galbraith, R.F., 1981. On statistical models for fission-track counts. *J. Math. Geol.*, **13**, 471–478.

Galbraith, R.F. and Green, P.F., 1990. Estimating the component ages in a finite mixture. *Nucl. Tracks Radiat. Meas.*, **17**, 197–206.

Gallagher, K., Roderick, B. and Johnson, C., 1998. Fission track analysis and its applications to geological problems. *Annu. Rev. Earth Planet. Sci.*, **26**, 519–572.

Garver, J.I., Reiners, P.W., Walker, L.J., Ramage, J.R. and Perry, S.E., 2005. Implications for timing of Andean uplift from the thermal resetting of radiation-damaged zircon in the Cordillera Huayhuash, Northern Peru. *J. Geol.*, **113**, 117–138.

Ghiglione, M.C. and Cristallini, E.O., 2007. Have the southernmost Andes been curved since Late Cretaceous time? An analog test for the Patagonian Orocline. *Geology*, **35**, 13–16.

Ghiglione, M.C. and Ramos, V.A., 2005. Progression of deformation and sedimentation in the southernmost Andes. *Tectonophysics*, **405**, 25–46.

Ghiglione, M.C., Yagupsky, D., Ghidella, M. and Ramos, V.A., 2008. Continental stretching preceding the opening of the Drake Passage: evidence from Tierra del Fuego. *Geology*, **36**, 643–646.

Giacosa, R.E. and Heredia, N., 2004. Structure of the north Patagonian thick-skinned fold-and-thrust belt, southern central Andes, Argentina (41º-42ºS). *J. S. Am. Earth Sci.*, **18**, 61–72.

Gombosi, D.J., Barbeau, D.L., Hourigan, J.K. and Zhao, D., 2008. Mircoprobe assisted zoned alpha corrections in zircon (U-Th)/He chronology. *Proceedings from the 11th International Conference on Thermochronometry*, 12-19 September, Anchorage Alaska, 110 pp.

Hervé, F., Fanning, C.M. and Pankhurst, R.J., 2003. Detrital zircon age patterns and provenance of the metamorphic complexes of southern Chile. *J. S. Am. Earth Sci.*, **16**, 107–123.

Hervé, F., Pankhurst, R.J., Fanning, C.M., Calderón, M. and Yaxley, G.M., 2007. The south Patagonian batholith: 150 My of granite magmatism on a plate margin. *Lithos*, **97**, 373–394.

Hervé, F., Calderón, M. and Faúndez, V., 2008. The metamorphic complexes of the Patagonian and Fuegian Andes. *Geol. Acta*, **6**, 43–53.

Hourigan, J.K., Reiners, P.W. and Brandon, M.T., 2005. U-Th zonation-dependent alpha-ejection in (U-Th)/He chronometry. *Geochim. Cosmochim. Acta*, **69**, 3349–3365.

House, M.A., Farley, K.A. and Stockli, D., 2000. Helium chronometry of apatite and titanite using Nd-YAG laser heating. *Earth Planet. Sci. Lett.*, **183**, 365–368.

Hurford, A.J. and Green, P.F., 1983. The zeta age calibration of fission-track dating. *Isot. Geosci.*, **1**, 285–317.

Kennett, J.P., 1977. Cenozoic evolution of Antarctic glaciation, the circum-Antarctic Ocean, and their impact on global paleooceanography. *J. Geophys. Res.*, **82**, 3843–3860.

Ketcham, R.A., 2005. Forward and inverse modeling of low-temperature thermochronometry data. In: *Low-Temperature Thermochronology: Techniques, Interpretations, and Applications* (P.W. Reiners and T.A. Ehlers, eds), *Rev. Mineral. Geochem.*, **58**, 49–94.

Ketcham, R.A., Donelick, R.A. and Carlson, W.D., 1999. Variability of apatite fission-track annealing kinetics: III. Extrapolation to geological time scales. *Am. Mineral.*, **84**, 1235–1255.

Klepeis, K.A., 1994a. Relationship between uplift of the metamorphic core of the southernmost Andes and shortening in the Magallanes foreland fold and thrust belt, Tierra del Fuego, Chile. *Tectonics*, **13**, 882–904.

Klepeis, K.A., 1994b. The Magallanes and Deseado fault zones: major segments of the South American-Scotia transform plate boundary in southernmost South America, Tierra del Fuego. *J. Geophys. Res.*, **99**, 22001–22014.

Klepeis, K.A. and Austin, J.A.A., 1997. Contrasting styles of superposed

deformation in the southernmost Andes. *Tectonics*, **16**, 755–776.
Klepeis, K., Betka, P., Alverez, J., Poblete, F., Thomson, S., Gehrels, G. and Clarke, G., 2008. Tectonic evolution of a doubly-vergent, thick-skinned fold and thrust belt in the Patagonian Andes, southernmost South America. *Geol. Soc. Am. Abstr. Prog.*, **40**, 548.
Kohn, M.J., Spear, F.S. and Dalziel, I.W.D., 1993. Metamorphic P-T paths from Cordillera Darwin, a core complex in Tierra del Fuego, Chile. *J. Petrol.*, **34**, 519–542.
Kohn, M.J., Spear, F.S., Harrison, T.M. and Dalziel, I.W.D., 1995. $^{40}Ar/^{39}Ar$ geochronology and P-T-t paths from the Cordillera Darwin metamorphic complex, Tierra del Fuego, Chile. *J. Metamorph. Geol.*, **13**, 251–270.
Kraemer, P.E., 2003. Orogenic shortening and the origin of the Patagonian orocline (56º S. Lat). *J. S. Am. Earth Sci.*, **15**, 731–748.
Lagabrielle, Y., Goddéris, Y., Donnadieu, Y., Malavieille, J. and Suarez, M., 2009. The tectonic history of Drake Passage and its possible impacts on global climate. *Earth Planet. Sci. Lett.*, **279**, 197–211.
Lawver, L.A. and Gahagan, L.M., 2003. Evolution of Cenozoic seaways in the circum-Antarctic region. *Palaeogeogr. Palaeoclimatol. Palaeoecol.*, **198**, 11–37.
Livermore, R., Nankivell, A., Eagles, G. and Morris, P., 2005. Paleogene opening of the Drake Passage. *Earth Planet. Sci. Lett.*, **236**, 459–470.
Livermore, R., Hillenbrand, C.D., Meredith, M. and Eagles, G., 2007. Drake Passage and Cenozoic climate: an open and shut case? *Geochem. Geophys. Geosyst.*, **8**, Q01005.
Marshak, S., 1988. Kinematics of orocline and arc formation in thin-skinned orogens. *Tectonics*, **7**, 73–86.
Menichetti, M., Lodolo, E. and Tassone, A., 2008. Structural geology of the Fuegian Andes and Magallanes fold-and-thrust belt – Tierra del Fuego Island. *Geol. Acta*, **6**, 19–42.
Mukasa, S.B. and Dalziel, I.W.D., 1996. Southernmost Andes and South Georgia Islands, North Scotia Ridge: zircon U-Pb and muscovite $^{40}Ar/^{39}Ar$ age constraints on tectonic evolution of Southern Gondwanaland. *J. S. Am. Earth Sci.*, **9**, 349–365.
Nelson, E.P., 1982. Post-tectonic uplift of the Cordillera Darwin orogenic core complex: evidence from fission-track geochronology and closing temperature-time relationships. *J. Geol. Soc. Lond.*, **139**, 755–761.
Nelson, E.P., Dalziel, I.W.D. and Milnes, A.G., 1980. Structural geology of the Cordillera Darwin-collision style orogenesis in the southernmost Andes. *Eclogae Geol. Helv.*, **73**, 727–751.
Olivero, E.B. and Malumián, N., 2008. Mesozoic-Cenozoic stratigraphy of the Fuegian Andes, Argentina. *Geol. Acta*, **6**, 5–18.
Pankhurst, R.J., Riley, T.R., Fanning, C.M. and Kelley, S.P., 2000. Episodic silicic volcanism in Patagonia and the Antarctic Peninsula: chronology of magmatism associated with the break-up of Gondwana. *J. Petrol.*, **41**, 605–625.
Rapalini, A.E., 2007. A paleomagnetic analysis of the Patagonian Orocline. *Geol. Acta*, **5**, 287–294.
Regüero, M.A., Marenssi, S.A. and Santillana, S.N., 2002. Antarctic Peninsula and South America (Patagonia) Paleogene terrestrial faunas and environments: biogeographic relationships. *Paleogeogr. Paleoclimatol. Paleoecol.*, **179**, 189–210.
Reiners, P.W. and Nicolescu, S., 2006. Measurement of parent nuclides for (U-Th)/He chronometry by solution sector ICP-MS. ARHDL Report 1. Available at: http://www.geo.arizona.edu/~reiners/arhdl/arhdl.htm. (last accessed 01 November 2009)
Reiners, P.W., Brady, R., Farley, K.A., Fryxell, J.E., Wernicke, B.P. and Lux, D., 2000. Helium and argon thermochronometry of the Gold Butte block, South Virgin Mountains, Nevada. *Earth Planet. Sci. Lett.*, **178**, 315–326.
Reiners, P.W., Spell, T.L., Nicolescu, S. and Zanetti, K.A., 2004. Zircon (U-Th)/He thermochronometry: He diffusion and comparisons with $^{40}Ar/^{39}Ar$ dating. *Geochim. Cosmochim. Acta*, **68**, 1857–1887.
Scher, H.D. and Martin, E.E., 2006. Timing and climatic consequences of the opening of Drake Passage. *Science*, **312**, 428–430.
Somoza, R., 1998. Updated Nazca (Farallon)-South America relative plate motions during the last 40 m.y.: implications for mountain building in the central Andean region. *J. S. Am. Earth Sci.*, **11**, 211–215.
Somoza, R. and Ghidella, M.E., 2005. Convergencia en el margen occidental de América del Sur durante el Cenozoico: subducción de las placas de Nazca, Farallón y Aluk. *Rev. Asoc. Geol. Argent.*, **60**, 797–809.
Spotila, J.A., 2005. Applications of low-temperature thermochronometry to quantification of recent exhumation in mountain belts. In: *Low-Temperature Thermochronology: Techniques, Interpretations, and Applications* (P.W. Reiners and T.A. Ehlers, eds), *Rev. Mineral Geochem.*, **58**, 449–466.
Suárez, M. and Pettigrew, T.H., 1976. An Upper Mesozoic island-arc-back-arc system in the southern Andes and South Georgia. *Geol. Mag.*, **113**, 305–400.
Thomson, S.N., Hervé, F. and Stöckhert, B., 2001. Mesozoic-Cenozoic denudation history of the Patagonian Andes (southern Chile) and its correlation to different subduction processes. *Tectonics*, **20**, 693–711.
Torres Carbonell, P.J., Olivero, E.B. and Dimieri, L.V., 2008. Structure and evolution of the Fuegian Andes foreland thrust-fold belt, Tierra del Fuego, Argentina: paleogeographic implications. *J. S. Am. Earth Sci.*, **25**, 417–439.
Wilson, T.J., 1991. Transition from back-arc to foreland basin development in the southernmost Andes: stratigraphic record from the Ultima Esperanza District: Chile. *Geol. Soc. Am. Bull.*, **103**, 98–111.

Received 13 January 2009; revised version accepted 24 August 2009

Supporting Information

Additional Supporting Information may be found in the online version of this article:

Appendix S1 Fuegian Andes thermochronology sample locations, Argentina and Chile.

Appendix S2 Detailed analytical and modelling methods.

Appendix S3 Weighted zeta mean calibrations for zircon fission-track analysis, David J. Gombosi.

Appendix S4 Zircon fission-track raw data.

Appendix S5 Apatite fission-track age data for sample ROM-2G.

Appendix S6 Apatite fission-track track length data for ROM-2G.

Appendix S7 Raw data for apatite (U–Th–Sm)/He age calculations of standards and unknowns.

Appendix S8 Raw data for zircon (U–Th–Sm)/He age calculations of standards and unknowns.

Please note: Wiley-Blackwell is not responsible for the content or functionality of any supporting materials supplied by the authors. Any queries (other than missing material) should be directed to the corresponding author for the article.

